HIGH FREQUENCY PROPERTIES OF ALL-NbN NANOBRIDGES WITH GAP STRUCTURE IN I-V CURVES

K.Hamasaki, T.Yakihara, Z.Wang, T.Yamashita and *Y.Okabe
Department of Electronics, Technological University of Nagaoka, Kamitomioka 1603, Nagaoka 940-21, Japan
*Department of Electrical and Electronic Engineering, The University of Tokyo, 3-1, Hongo 7 chome, Bunkyoku, Tokyo 113, Japan

ABSTRACT

All-NbN nanobridges with gap structure in I-V curves have been reproducibly constructed using RIE and lift-off techniques. The nanobridges had a width of 2 μm, and a thickness of<30 nm. The length of nanobridge was about of the order of 3 to 5 coherence length of epitaxial NbN films. The nanobridges had nearly ideal characteristics: sharply defined critical current, high resistance, well-defined gap structure at about 4 mV, large I_cR_N products of ~3 mV, and low excess current. Small-area dc SQUIDs were made using the nanobridges, and analyses of the response to magnetic flux were performed. The current-phase relationship of the nanobridges was found to be close to sinusoidal. The maximum LC resonant voltage was about 1.2 mV, corresponding to a frequency of 580 GHz. The IF peak was obtained up to the bias voltage of about 4 mV in 101 GHz Josephson mixing.

INTRODUCTION

Attempts at mixing with Josephson bridges have resulted in very large conversion losses, mostly due to poor coupling from the signal source to the low-impedance junctions. The most successful device has usually been the high impedance point-contact Josephson junctions.[1,2] In their present form, these devices are probably not sufficiently stable for field applications. The rapidly developing technology of thin-film Josephson nanobridges may provide solutions to this problem.

The situation is, however, complex for the Josephson bridges due to the variety of structures, the diversity of experimental results and the different mechanisms(variation of the order parameter in time and space, vortex motion, and excess current). The physical picture of the excess current in particular is not clear although a few theoretical models were proposed.[3] In our research we attempted to produce Josephson nanobridges which have the same DC and RF properties as point-contact junctions.[4,5] Recently we developed all-NbN edge-junction nanobridges that show remarkable improvements in their Josephson characteristics compared to previous attempts.[6]

In this paper we will discuss the fabrication approaches which have been developed for producing Josephson nanobridges with gap structure and with high impedance. Then we present our preliminary results on Josephson mixing with such nanobridges. We will also discuss the Blonder model[7] and granular effect [8] to explain the origin of the gap-structure which is observed in our nanobridges.

FABRICATION TECHNIQUE

The NbN nanobridges can be prepared by RIE and lift-off techniques. The banks were produced using epitaxial NbN films with high critical temperatures and with substantially low resistivity. On the other hand, grany NbN films with high resistivity was used for the bridges. The epitaxial NbN films used in this work was developed by the authors.[9] Briefly, it consists of sequential deposition of highly oriented MgO and superconducting NbN films by RF magnetron sputtering.

The fabrication procedure as shown in Fig.1 is as follows : (a),(b) MgO and NbN films were sequentially sputter deposited onto the substrate at about 210 ℃. Next, the NbN was patterned by conventional photolithography and reactive ion etching to define the first bank.

(c),(d) A thin layer(10-20 nm) of MgO was deposited to define the bridge length, and then, without breaking the vacuum, a NbN film(130 nm) was sputter deposited at 60-90 ℃. After reactive ion etching to define the second bank, AZ resist was lifted off. In this step, all edge junctions showed high resistance (>M Ω) at 4.2 K, and there was no supercurrent. After the banks(edge-junction) were prepared, the surfaces of the banks were lightly sputter cleaned, and then a 30 nm film of NbN was deposited in Ar+(9-10 %)N_2 mixture. Finally a nanobridge dc SQUID was fabricated by reactive ion etching. This structure is similar to variable thickness bridge configuration.

The effects of Joule heating pose the primary limit on the performance of a nanobridge, and it is difficult thereafter to reliably measure the normal resistance. The MgO has very high thermal conductivity below 20 K, the same as diamond.[10] Hence it permits fast decay of Joule heating in the bridge region.

When the RIE and lift-off techniques are used to fabricate all-NbN edge-junction nanobridges, one problem is encountered which stems from the fact that the bridge and banks are not made of a single material. It results in the non eveness of edge-junctions. Unfortunately we can not control the shape of the edge junction thoroughly. However, roughness of the edge junctions, indeed, caused the grainy NbN films with high resistivity, and consequently nanobridges had good electrical characteristics as shown later.

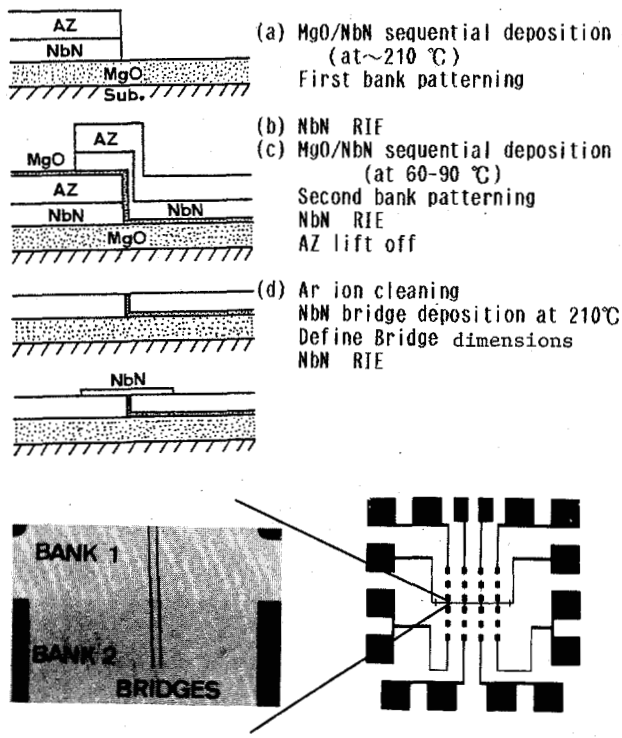

Fig.1 Fabrication sequence for all-NbN nanobridges using the RIE and lift-off techniques, and micrographs of mixer chip. The substrate is silicon or fused quartz.

Manuscript received October 12, 1986.

RESULTS AND DISCUSSION

The superconducting transitions were monitored resistively, and the temperature measured with a germanium resistance thermometer(Lake Shore Cryo., Inc. GR-200A). The resistance as a function of temperature for a typical nanobridge is shown in Fig.2. The critical current of this nanobridge dc-SQUID was about 30μA. Figure 2 clearly shows three transitions, one at ~11 K associated with the bridge, and the other 16 K and 14.8 K associated with the first and second banks, respectively.

The transition of bridge is broad, with an onset at about 13 K and a very long tail merging with ~10.3 K transition. The evaluated residual resistivity, ρ_0(14 K)= R(14 K)·W·d/L_B, for the bridge was~7000$\mu\Omega$·cm by using W=2 μm, d=30 nm, and L_B~20 nm as the thickness of MgO insulator. This value is much larger than that of epitaxial NbN films. It may probably be caused by the roughness of the edge-junction. Although we were not successful in controlling the resistivity of the bridge layer and the flatness in edge-junctions, we still believe that the grany NbN films ought to be used to prepare the high-impedance devices. The length of the bridge also must be of the order of 1-5 coherence length in order to obtain a well-developed Josephson effect, and the width should be of the order of the thin-film penetration depth $\lambda_\perp$ to reduce the kinetic inductance without reduction of normal resistance of nanobridges.

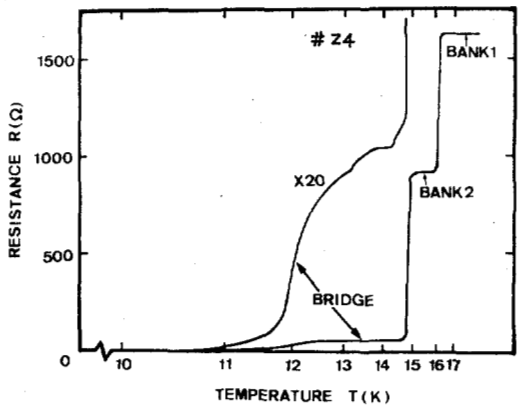

Fig.2 A typical superconducting-to-normal transition in the all-NbN nanobridge SQUID. The thickness of both banks is~150 nm, and bridge is ~30 nm.

Fig.3(a) shows the current-voltage(I-V) characteristics and the dynamic conductance of typical nanobridge SQUIDs without microwave. Note the well-defined gap structure at 4 mV. In all nanobridges fabricated, the voltage of the gaps was nearly 4 mV. The nanobridge also has a substantially high impedance, R_N~100 Ω, which results in easy coupling between the RF signal source and devices.

The clear gap structures first observed in all our NbN nanobridges may result from the extremely short length of bridge and the use of grany NbN film in bridge layer. The sharp I-V characteristics are similar to those for the high-quality point-contact junction. In addition the LC resonant steps are shown in Fig.3(a). The maximum resonant voltage V_{r2} observed was 1.2 mV, corresponding to a Josephson frequency of 580 GHz.

A more informative plot of the dependence of the critical current on external field was obtained, as shown in Fig. 3(b). Results indicated a nearly(if not exactly) sinusoidal current-phase relation from T_c to 4.2 K.

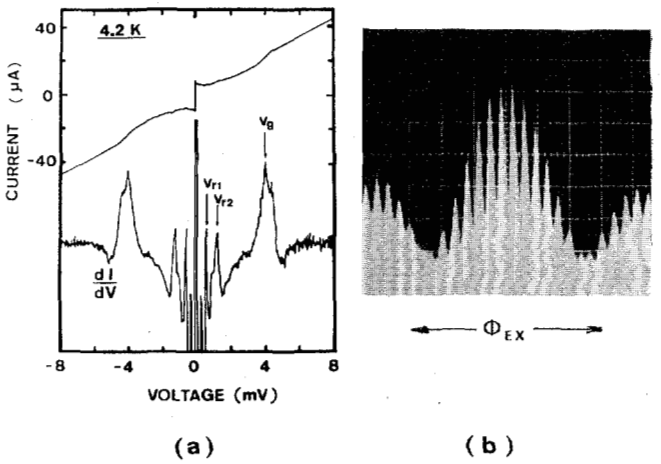

Fig.3 (a) I-V characteristic and dynamic conductance of a all-NbN nanobridge SQUID,
(b) Quantum interference pattern.

Fig.4(a) shows a set of I-V characteristics for our high-impedance nanobridge. The dependence of the excess current and critical current on temperature is shown in Figure 4(b). One evidence for Josephson coupling of grain is given by the temperature dependence of I_c near T_c. Near T_c, nanobridges tend to obey a more linear dependence on temperature, as $I_c \sim T_c - T$, that is, they obey the Josephson theory. In general, most of our high-impedance nanobridge had linear I_c-vs-T curves at near T_c. Very low-impedance and large-current nanobridges including non-Josephson current, of course, tend not to obey the Josephson theory.

The definition of the excess current is the same as reference[7]. Except for temperatures extremely close to T_c, this excess current is only weakly dependent on temperature. According to Blonder's theory which describes the crossover from metallic(SNS) to tunnel junction(SIS) behavior, the excess current on junctions has the temperature dependence of $I_{EX} \sim \Delta(T)$. In Fig.4(b)-(b), the experimental points fit the normalized curve of $\Delta(T)/\Delta(0)$ very well.

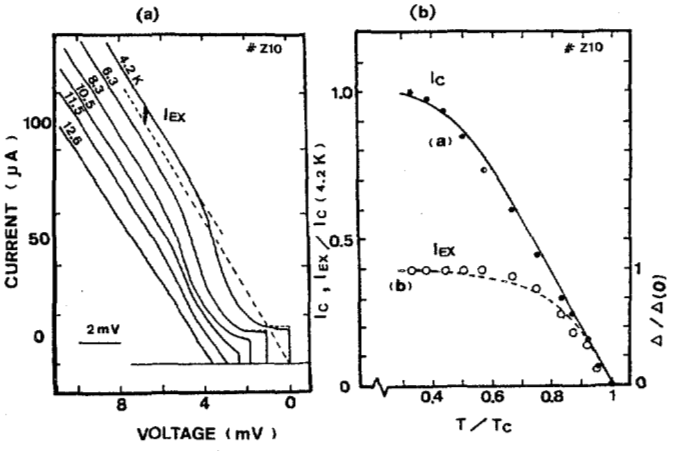

Fig.4 (a) I-V characteristics of a typical NbN nanobridge at different temperatures.
(b) Temperature dependence of normalized I_c and I_{EX} of a NbN nanobridge. The solid curve is theoretical dependence with experimental values indicated by circles, and dashed one is temperature dependence of the energy gap $\Delta(T)$.

The obtained I_cR_N products vary over a considerable range among the fabricated nanobridges. In Fig.5, I_c is plotted versus R_N for many nanobridges with gap at~4 mV. In all samples the thickness of bridge was about 30 nm. The differential resistance just above the gap is taken as a measure of the resistance, R_N, of the junction. In Blonder's model,[7] this definition gives a slight low value of R_N, even in the absence of heating effect.

For the samples with a critical current larger than 100 μA, I_cR_N products are higher than the tunnel limit. However, the R_N values for samples with large I_c are no longer true because of heating effect. For $I_c < 50\mu$A, it gave the I_cR_N products close to the theoretical value of tunnel limit, and all the nanobridges had very low excess current. For very low critical currents, $I_c < 10\mu$A, this product is generally less than the tunnel limit, mostly owing to suppression of I_c by thermal noise or self-field limiting. More detailed investigations should be conducted for flux trapping and noise suppression in I_c, and also for the constrictly definition of R_N.

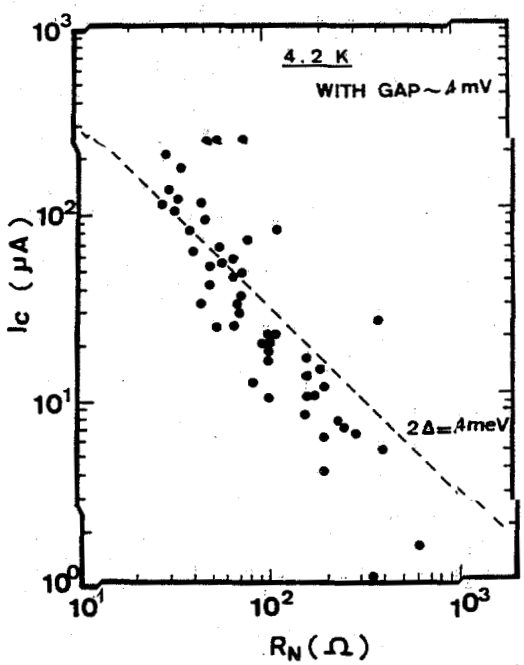

Fig.5 Plot of the I_c versus the normal resistance R_N for many nanobridge(dc SQUID) at 4.2 K. For all samples the thickness of bridge is about 30 nm.

As mentioned above, the initial layer of the bridge was about 30 nm in thickness. It is about seven times as thick as the coherence length of epitaxial NbN(ξ_{GL}~4.5 nm). Fig.6 shows the variation of I_c and R_N for two nanobridges, as the thickness of bridges were thinned by Ar ion etching. Some I-V characteristics are shown in this figure. The as prepared nanobridges have high excess current and faintish gap structure at about 4 mV(inset(a)). Then the bridge layer was reduced in thickness by Ar ion sputter etching at about 0.15 W/cm² RF power density. The I-V curve(inset(c)) with the critical current of about one tenth of the initial value(a) shows the well-defined gap structure at~4 mV. Note that the excess current is decreased as the thickness of the bridge was reduced to ξ or thereabout. When the bridge was thoroughly etched out, the edge junctions show high impedance (>M Ω) as in inset (d). In this experiment, high RF-power density in sputter etching caused insulation breakdown in NbN edge junctions.

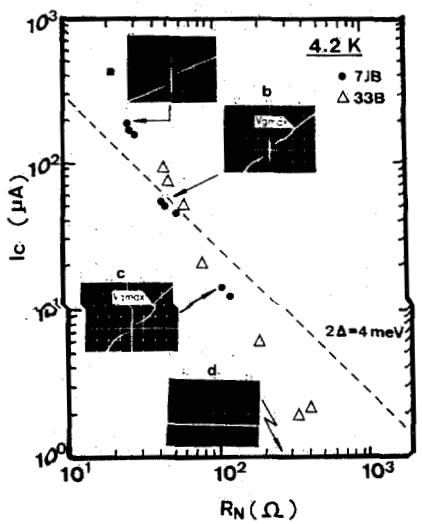

Fig.6 Plot of the I_c versus the R_N for two nanobridge SQUID at 4.2 K. Some I-V curves are shown in this figure. The bridges were thinned by sputter etching in Ar.

The millimeter wave responce of a high-impedance NbN nanobridge is shown in Fig.7. The well-pronounced current steps have been observed up to~2.5 mV with 10^1 GHz radiation, indicating that heating effect is not a problem in these nanobridges. Also, it can be seen that the induced steps show no evidence of subharmonic structure, contrary to the vortex model prediction.

This and the high normal resistances of these nanobridges(~100 Ω) may enable practical applications for bridges.

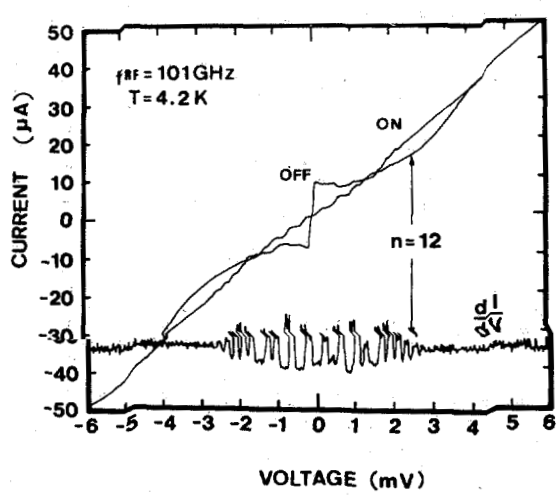

Fig.7 I-V characteristic and dynamic conductance of a nanobridge SQUID without RF and with RF power at 101 GHz.

Figure 8 shows the mixer chips and preliminary result in Josephson mixing. The geometry was designed for testing them as mixers at 101 GHz so the nanobridges are located at the center of a stripline choke structure. The static I-V curves with and without LO power and IF output for fundamental mixing are plotted as a function of voltage for a nanobridge SQUID. It was operated at T=4.2 K with f_{IF}=4 GHz.

The IF peak is obtained up to the bias voltage of about 4 mV, corresponding to gap voltage of NbN nanobridges. The RF coupling is poor because the thin film antenna structure was not optimized. It is, however, possible that careful attention to improving the coupling characteristics may provide further significant improvements in nanobridge performance at high frequencies. Mixer experiment was carried out at the Radio Research Laboratory, Ministry of Posts & Telecom., Japan. The detailed results will be reported in this conference by our co-worker.

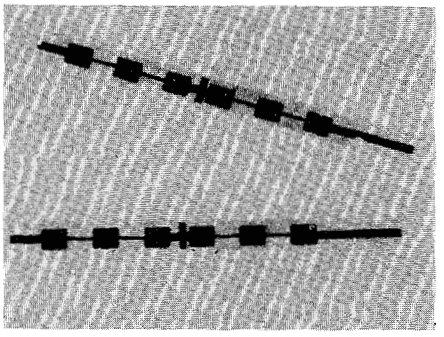

(a)

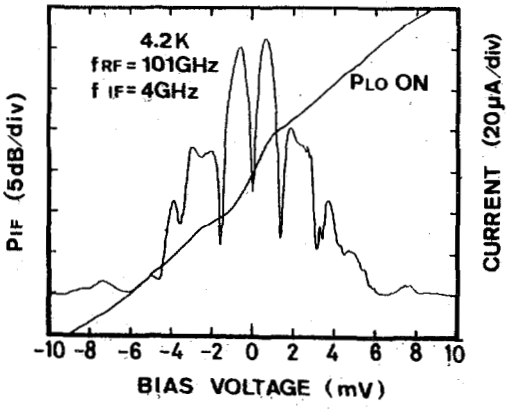

(b)

Fig.8 (a) Complete nanobridge SQUID and choke structure.
(b) I-V characteristics and IF output with external LO at 105 GHz for an all-NbN nanobridge at 4.2 K.

CONCLUSION

In this paper we reported the development of a new type of thin film nanobridge that shows remarkable improvements in its Josephson characteristics compared to previous attempts. They had good electric characteristics : sharply defined critical current, high impedance, well-defined gap structure, large I_CR_N products, and low excess current. In the present high-impedance nanobridges, the good agreement between experiment and theory for curves $I_C(T)$ and $I_{EX}(T)$ also indicated that the observed superconducting current is actually a tunnel current, and does not owe its origin to superconducting metal contacts between banks. The nanobridge SQUID without excess current had nearly ideal depth of the flux modulation. The LC resonant steps up to 1.2 mV were also observed in I-V curves. The IF peak was obtained up to the bias voltage of about 4 mV in 101 GHz Josephson mixing. The well-defined gap structure and high impedance in the present nanobridges may permit high performance as Josephson mixer at high frequencies.

ACKNOWLEDGEMENT

Part of the present work was financially supported by the Grant-in-Aid for new digital integrated circuit with bridge Josephson junctions from the Ministry of Education of Japan. The authors would like to thank Dr.Matsui for his support of this research and helpful discussions. We are grateful to M.Nishino for his help in our experiments.

REFERENCES

[1] Y.Taur and A.R. Kerr; Appl. Phys. Lett., 32,775 (1978)
[2] J.H.Classen and P.L.Richards; J. Appl.Phys., 49 4130 (1978), J.H.Classen and P.L.Richard; J. Appl. Phys., 49 4117 (1978)
[3] K.K. Likharev; Rev. Mod. Phys., 51 101 (1979)
[4] K.Hamasaki, K.Matsumoto, Y.Kodaira, T.Komata and T.Yamashita; The Trans. IECE of Jpn., E67, 123 (1984)
[5] T.Yamashita, K.Hamasaki, Y.Kodaira and T.Komata; IEEE Trans on Magn., MAG-21, 932 (1985)
[6] T.Yakihara, K.Hamasaki, T.Yamashita, T.Matsui and R.Hayashi; Trans IECE Japan, E69, 427 (1986)
[7] G.E. Blonder, M.Tinkham, T.M.Klapwijk; Phys.Rev.B, 25 4515 (1982), T.M.Klapwijk, G.E.Blonder and M.Tinkham; Physica 109&110B, 1657 (1982)
[8] J.H.Claassen; Appl. Phys. Lett., 40, 839 (1982)
[9] T.Yamashita, K.Hamasaki and T.Komata; Adv. Cryog. Mate. Vol.32 (1986) To be published
[10] Thermal Conductivity Nonmetalic Solids, The TRPC Data Series Vol.2, ed. Y.S.Touloukian(IFI/Plenum, New York, (1970)
[11] V.Ambegaokar and A.Baratoff ; Phys. Rev. Lett., Vol.10, 479 (1963)